Alloy Structures of the Ti-Ni-Ru System in the Ti-TiNi-TiRu Composition Range

By E. L. Semenova and N. Yu. Krendelsberger

I. N. Frantsevich Institute for Problems of Materials Science, NAS of Ukraine, 3, Krzhyzhanovsky str., Kiev, 03142, Ukraine

Interest in the alloys of the titanium-nickel system is due to their attractive properties: the high strength of nickel-based alloys, the ability of intermediate phases based on Ti_2Ni and TiNi to undergo amorphisation and hydrogen absorption, and the thermoelasticity of TiNi-based alloys. Ti-Ni alloys are resistant to oxidation and corrosion in most mild corrosive environments, and are used in chemical, medical and engineering applications. Here, we report on alloys in the Ti-TiNi-TiRu composition range of the Ti-Ni-Ru system, where ruthenium additions produce some interesting effects. Using phase diagrams and experimental results, the constituents of high temperature alloys and alloying processes are discussed.

An important aim of modern metals science is to create new alloys with specific properties. The interest in the ternary and multicomponent alloys of the titanium-nickel (Ti-Ni) system lies in their properties: high strength nickel-based alloys, intermediate phases based on Ti_2Ni and TiNi which undergo amorphisation and hydrogen absorption, and thermoelasticity in TiNi-based alloys. Ti-Ni alloys are resistant to oxidation and corrosion, so are used in chemical plants, medical devices and equipment, and underwater engineering.

However, when ruthenium is added to titanium-based alloys and intermediate phases of the Ti-Ni system, the resulting Ti-Ni-Ru ternary alloys show superior corrosion properties (1). Ruthenium-enhanced α, $\alpha+\beta$, and β titanium alloys display high corrosion resistance in dilute acids and hot brine environments (2). Adding ruthenium to some nickel-containing steels improves their corrosion resistance (3). Such ternary alloys may be able to improve on other characteristics of the binary alloys.

In studying alloy properties and in developing new materials, information on phase diagrams is needed. Phase diagrams help in interpreting properties and may contribute to understanding process mechanisms, such as corrosion. They also allow properties to be correlated with alloy composition and temperature. Here, we examine the Ti-TiNi-TiRu system and report some exciting effects due to ruthenium. As the number of published papers on ruthenium seems to be growing (4), we hope this paper will contribute to the interest, and help in the search and development of new materials.

Information on the Ti-Ni-Ru system is fragmentary and contradictory. Our earlier studies of ternary Ti-Ni-Ru alloys along the TiNi-TiRu section showed that TiNi and TiRu form a continuous solid solution at the subsolidus temperatures (5, 6). We believe this will affect many aspects of the Ti-Ni-Ru phase diagram. Taking the solid solution between TiNi and TiRu into account, the phase equilibria in the Ti-Ni-Ru ternary system are expected to be different from those which would occur if the TiNi-TiRu section was peritectic (7, 8), although interpreting the TiNi-TiRu system as peritectic is inaccurate (5). Phase diagrams of the Ti-Ru and Ti-Ni binary boundary systems up to 50 at.% Ni are well known (9), the main features are:

Ti-Ru System

The equiatomic phase (δ) in the Ti-Ru system has a CsCl-type cubic crystal structure and crystallises from the melt at 2160 $\pm$ 50°C. It is stable down to room temperature. It is homogeneous over the range 45 to 51 at.% Ru at 1575°C.

The β-phase, based on titanium, crystallises from the melt into alloys which can contain up to 24 at.% Ru. In the range ~ 24–45 at.% Ru the β-phase is formed by peritectic reaction, at 1575°C, and coexists as a solid with the δ-phase ($\beta+\delta$)

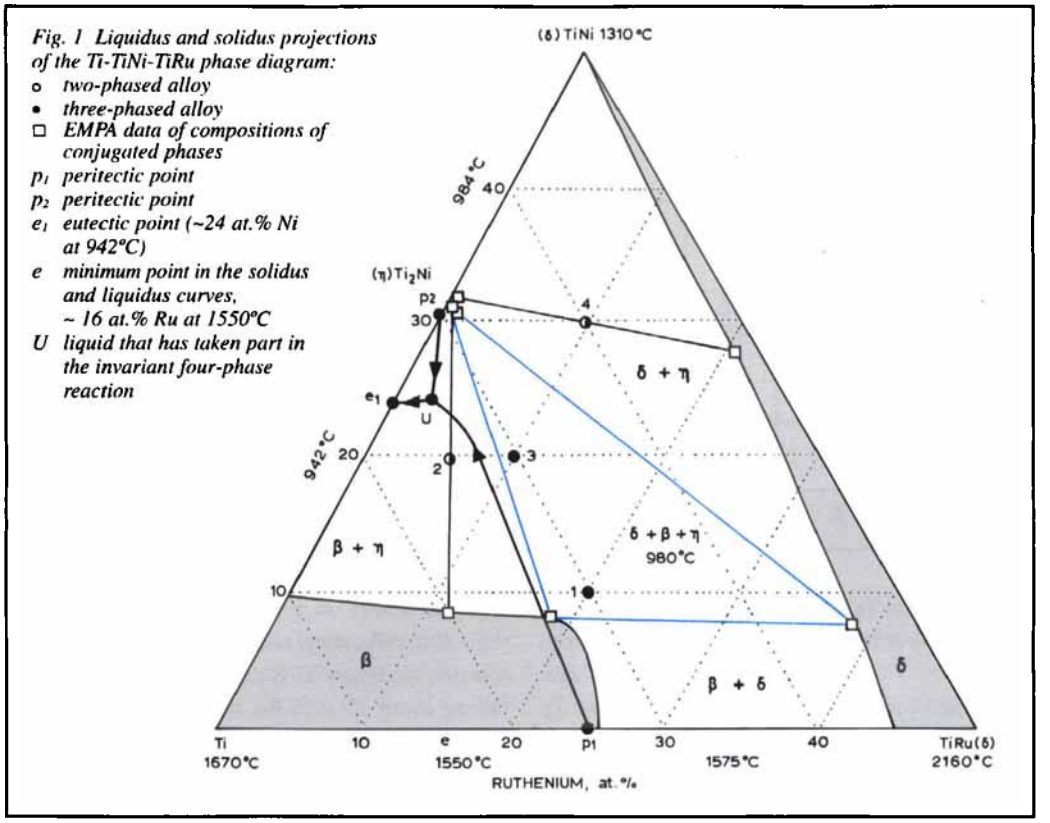

Fig. 1 Liquidus and solidus projections of the Ti-TiNi-TiRu phase diagram:
- o *two-phased alloy*
- • *three-phased alloy*
- □ *EMPA data of compositions of conjugated phases*

p_1 *peritectic point*
p_2 *peritectic point*
e_1 *eutectic point (~24 at.% Ni at 942°C)*
e minimum point in the solidus and liquidus curves, ~ 16 at.% Ru at 1550°C
U liquid that has taken part in the invariant four-phase reaction

alloys. However, at 24–25 at.% Ru, an interval of ~ 1 at.%, the product of the reaction is β-phase in solid.

Ti-Ni System

The TiNi-based δ-phase crystallises from the melt at 1310°C. The titanium solubility in the δ-phase is < 1 at.%. The phase based on Ti_2Ni (η) is formed by the peritectic reaction $\delta + L \leftrightarrow \eta$ at 984°C. L is liquid at peritectic point p_2 (~ 31 at.% Ni). The η-phase forms a eutectic with the β-phase at 942°C. At the eutectic point, e_1, the alloy contains ~ 24 at.% Ni. Nickel solubility in titanium is ~ 10 at.% at the subsolidus temperature.

Production of the Ti-Ni-Ru Phase Diagram

Starting materials for the synthesis of the Ti-Ni-Ru alloys were: ruthenium powder (99.95 mass%), nickel (99.99 mass%) and iodised titanium (99.98 mass%). Alloy preparation and surface etching have been described (2). The alloys were annealed at subsolidus temperatures, 900 to 930°C, and as-cast and annealed specimens were studied. The electron microprobe analysis method (EMPA) was used to determine the composition of the conjugated phases, besides the investigations mentioned in (5).

Results and Discussion

From our investigation on Ti-Ni-Ru alloys, new data on phase equilibria in the system at subsolidus temperature and on alloy crystallisation were obtained first.

No ternary compounds were found in the Ti-Ni-Ru system, so the equilibria in the system are determined by intermediate phases based on compounds in the binary boundary systems and solid solutions based on the components. The vertical section between the TiNi and TiRu equiatomic compounds (isopleth) for 50 at.% Ti is quasibinary and allows the Ti-Ni-Ru system to be triangulated into two thermodynamically indepen-

Table I

Alloy Phase Composition and the Solidus Temperature

Alloy composition, at.%		Primary phase	Heat treatment		Phase composition	Solidus temperature, T_{sol}, °C	Lattice parameters, nm		
			Temp.,	Time,			β	η	δ
Ni	Ru		T, °C	h			a	a	a
10	20	δ	900 930	24 5	δ+β+η	980	0.315	1.131	0.306
20	5	β	900 930	20 24	β+η	975	0.318	1.133	–
20	10	δ	900 930	24 5	δ+β+η	–	0.315	1.131	0.306
30	10	δ	900	28	δ+η	980	–	1.130	0.305

dent subsystems: Ti-TiNi-TiRu and TiNi-Ni-Ru-TiRu.

These two subsystems can be treated separately; the Ti-TiNi-TiRu subsystem is discussed here. Solidus and liquidus surface projections (Figure 1), based on experimental results (such as Figures 2 and 3 and Tables I and II), an isopleth (Figure 4) and a crystallisation scheme for the Ti-TiNi-TiRu alloys (Figure 5) have been constructed. The isothermal section at 700°C (Figure 6) is based upon experimental data at subsolidus temperatures, theory and data from the literature. Phases existing at solidus temperatures are described in Table I.

Solidus Surface of the Ti-TiNi-TiRu Subsystem

There is a wide range β-titanium-based solid solution at solidus temperature (Figure 1). The solubility of nickel (maximum ~ 10 at.%) in titanium depends weakly on the ruthenium content up to the 7.4Ni-18Ru alloy; after this it sharply decreases towards the binary Ti-Ru system, to the alloy containing about 25 at.% Ru, which is the maximum solubility of ruthenium in titanium.

The solidus temperature of the β-phase decreases through the mutual ruthenium/nickel solution from 1670°C (melting point of Ti) to 1575°C in the Ti-Ru binary system, then decreases again to 980°C in the ternary system to the 7.4Ni-18Ru alloy, which is a vertex of the δ+β+η-phase triangle. Further decreases in the ruthenium content in the β-phase (towards the binary Ti-Ni system) result in the solid solution temperature dropping to 942°C, the temperature of the eutectic reaction L ↔ β+η here.

Titanium solubility in the δ-phase increases

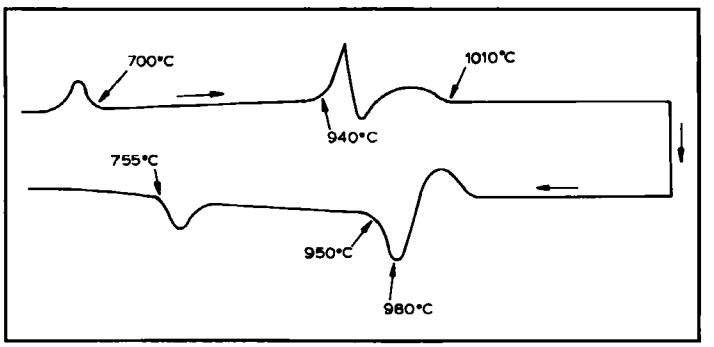

Fig. 2 DTA curves of titanium alloy 10Ni-20Ru (δ+η+β) and reference alloy 20Ni-80Ti (η+β). On heating, melting begins at ~ 940°C for 20Ni-80Ti, and near the peak of the curve for 10Ni-20Ru; at 1010°C solid-liquid state reactions end. On cooling, crystallisation begins at ~ 1020°C for 10Ni-20Ru and at ~ 1000°C for 20Ni-80Ti. At 980 and 950°C, respectively, the solid-liquid reactions end. At 700 (20Ni-80Ti) and 755°C, solid state reactions occur for Ti-based alloys

Table II

Composition of Phases at the Solidus Temperature in the Ti-TiNi-TiRu System

Alloy composition, at.%		Coexisting phases	Phase composition, at.%					
			β		δ		η	
Ni	Ru		Ni	Ru	Ni	Ru	Ni	Ru
10	20	δ+β+η	7.4	18	7	37	30.5	1
20	5	β+η	7	12	–	–	30.5	1
30	10	η+δ	–	–	27	20	32	1

gradually as nickel is replaced by ruthenium. The upper titanium border of the δ-phase in the ternary Ti-Ni-Ru system connects the points of the 50Ti-50Ni alloy and the 45Ru-55Ti alloy of the Ti-Ru binary system, corresponding to the maximum titanium solubility in Ti-Ru at subsolidus temperature (Figure 1). The solidus temperature of the δ-phase at the Ru-rich side is the lowest (980°C) at composition 7Ni-37Ru which is another of the vertices of the β+η+δ-phase triangle, see Table II.

In conformity with the solidus surface of the δ and β single-phase fields, a sharp fall was observed in the temperature of the β+δ ruled surface from 1575°C (the temperature of the peritectic horizontal in the binary Ti-Ru system) to 980°C (the solidus temperature of the δ+β+η alloy).

As the β+η alloy composition moves away from the side of the β+η+δ tie-line triangle towards the Ti-Ni face, the temperature of the β+η ruled surface drops. Comparable differential thermal analysis (DTA) data obtained for alloys from the β+η+δ region and from the binary Ti-Ni system confirm this (Figure 2). As Figure 2 shows, the binary alloy starts to melt at ~ 940°C. For the ternary alloy the onset of melting is near the peak of the curve but cannot be determined accurately because of the superimposition of thermal effects. At 1010°C the solid-liquid state reactions end.

Microprobe analysis of the annealed 20Ni-5Ru alloy (Figure 3a) show the compositions of the conjugated phases (light grains are η-phase, dark grains are β-phase) and indicate that the solubility of ruthenium in the η-phase does not exceed 1 at.%, while the solubility of nickel in the β-phase is ~ 3 at.% smaller than in the Ti-Ni binary system.

The temperature drops very slowly along the tie-lines that envelop the L+η+δ three-phase volume.

As mentioned before, the solidus temperature of the three-phase alloys, β+δ+η, is 980°C (Figure 1). The coordinates of the vertices of the tie-line triangle around the solidus surface of the β+δ+η phases are shown in Table II.

Thus the solidus surface of the Ti-TiNi-TiRu subsystem is formed by surfaces of three solid solutions based on β-titanium and on two intermediate phases (η and δ), by three ruled surfaces that terminate the two-phase solid regions (η+δ, δ+β, β+η) and by the plane of the tie-line triangle (β+δ+η).

Liquidus Surface of the Ti-TiNi-TiRu Subsystem

The liquidus surface of the Ti-TiNi-TiRu subsystem consists of three surfaces of primary crystallisation of δ-, η- and β-phases.

The δ-phase has the largest area, showing an extended range of concentrations; it has the largest region of primary crystallisation, bounded by p_1Up_2 (Figure 1). Microstructures of as-cast alloys from this region (Figures 3b, 3c and 3d) show the δ-phase displays coarse grains of varying composition in a dark matrix. The dark matrix is a mixture of phases that form on further cooling the ingots.

The microstructure of the 30Ni-10Ru alloy (Figure 3b) shows that the incongruent reaction of η-phase formation which took place in the Ti-Ni binary system is retained in the ternary system. Light grains of the δ-phase can be seen, with signs of a peritectic reaction along their edges resulting in

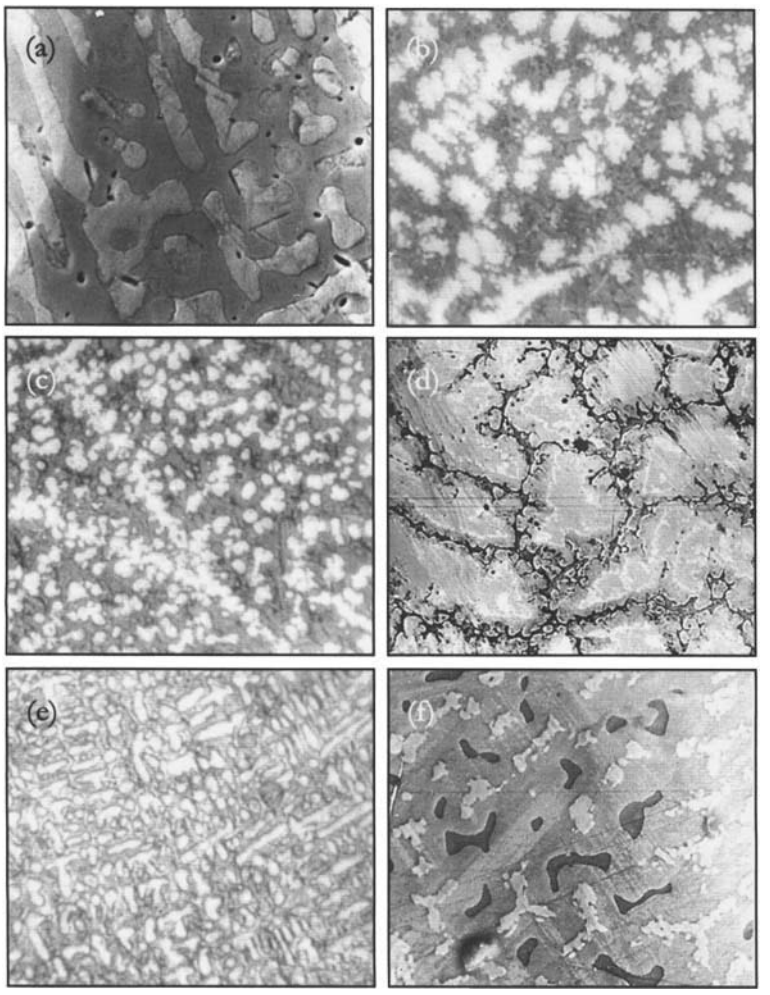

Fig. 3 SEM microstructures of the Ti-TiNi-TiRu alloys: (a) 20Ni-5Ru, annealed, β+η, × 800 (b) 30Ni-10Ru, as-cast, × 300 (c) 20Ni-10Ru, as-cast, × 400 (d) 10Ni-20Ru, as-cast, × 300 (e) 20Ni-5Ru, as-cast, × 400 (f) 10Ni-10Ru, annealed, δ+β+η, × 600

the formation of the η-phase (grey matrix). The η-phase lies between the δ-phase and liquid frozen in the very small (dark) interdendritic spaces.

The primary crystallisation of the δ-phase in the 20Ni-10Ru alloy (Figure 3c) is followed by common freezing of the β- and η-phases, according to four-phase invariant reaction: $L+\delta \leftrightarrow \beta+\eta$.

In Figure 1, the region of primary β-phase crystallisation is shown by the borders or monovariant curves: Up_1 and Ue_1. The incongruent reaction of β-phase formation which takes place in the Ti-Ru binary system is retained in the ternary system – up to alloy composition ~ 7Ni-18Ru, then (in the ternary system) the character of the β-phase crystallisation changes to a congruent one. The evidence for this is the different shape of the dendrite crystals of the δ- and β-phases in the 20Ni-10Ru and 20Ni-5Ru alloys, see Figures 3c and 3e, respectively, which lie along both sides of the monovariant curve p_1U.

The microstructure of the as-cast alloy containing 10Ni-20Ru (Figure 3d) shows the tendency of the δ-phase to overcool. Coarse light grains of the primary δ-phase can be seen, with small quantities of liquid freezing between them (the dark and very dark areas). A vertical section taken along the isoconcentrate (isopleth) 10 at.% Ni (Figure 4) has been constructed from the known characteristic temperature effects of this alloy (DTA) and from data obtained from the constitution of the boundary Ti-Ni and TiNi-TiRu phase diagrams (5, 9) and explains the microstructure.

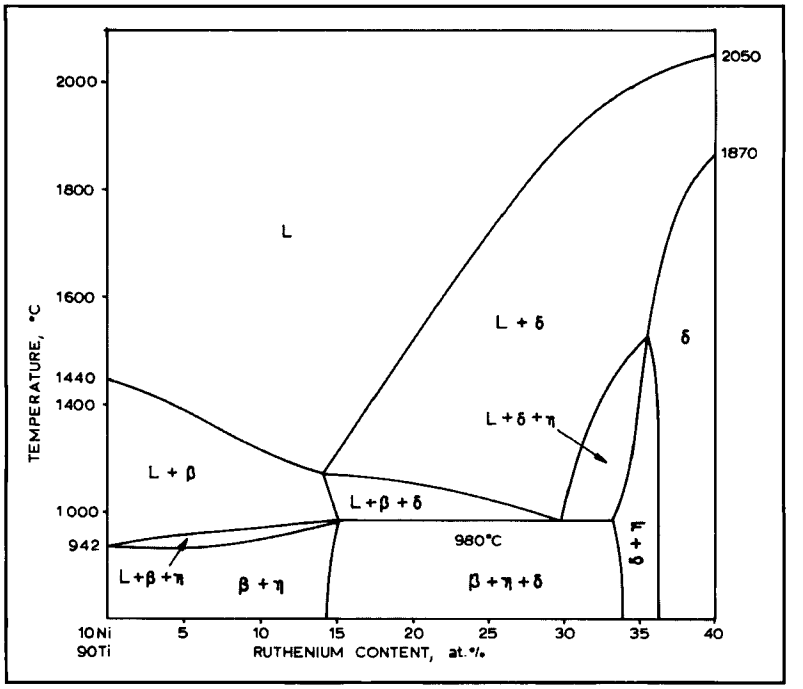

Fig. 4 Isopleth through the 10 at.% Ni isoconcentrate of the Ti-TiNi-TiRu phase diagram, showing processes taking place as the temperature changes, and showing the solidus and liquidus temperatures of the alloys. The isopleth passes through two fields of primary crystallisation of δ- and β-phases and crosses four three-phase regions, connected to the invariant four-phase transformation at 980°C (horizontal line). Two solid-phase regions: β+η and δ+η are seen. The temperature interval of the δ-phase crystallisation is large compared to the L+β+δ process, the latter is thus inhibited on rapid ingot cooling, resulting in microstructure of as-cast alloy with 10Ni-20Ru, shown in Fig. 3d

The large temperature range of the δ-phase primary crystallisation and the very narrow one for the following L ↔ η+β reaction results in non-equilibrium proportions of the phases present (Figures 3d and 4). On subsequent annealing, the 10Ni-20Ru alloy becomes a three-phase alloy (Figure 3f).

The composition range and field of primary crystallisation of the η-phase (Figure 1) e_1Up_2, is very small.

Monovariant processes L+δ ↔ η and L ↔ β+δ proceed to the invariant four-phase equilibrium reaction L+δ ↔ β+η which occurs at 980°C in this system (Figure 5.) The composition of the liquid at point 'U' taking part in this reaction is ~ 24Ni-2Ru, which is close to the liquid composition of the L ↔ β+η eutectic in the Ti-Ni binary system. Originating on the β+η side of the β+δ+η tie-line triangle, the L ↔ β+η monovariant process descends along the Ue_1 curve towards the Ti-Ni face to the lower temperature of 942°C.

Thus the processes occurring in the Ti-TiNi-TiRu system pass from the incongruent reactions observed in the Ti-Ni and Ti-Ru binary systems

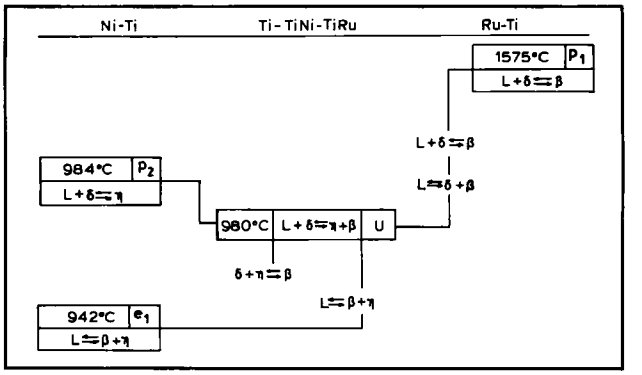

Fig. 5 Scheme of crystallisation of the Ti-TiNi-TiRu alloys, showing the binary and ternary invariant reactions which contribute to the four-phase peritectic equilibrium L+δ ↔ β+η. The two three-phase processes: L+δ ↔ β and L+δ ↔ η occur at higher temperatures than the four-phase process, followed by L ↔ β+η after its completion. Phase δ+η+β precipitates

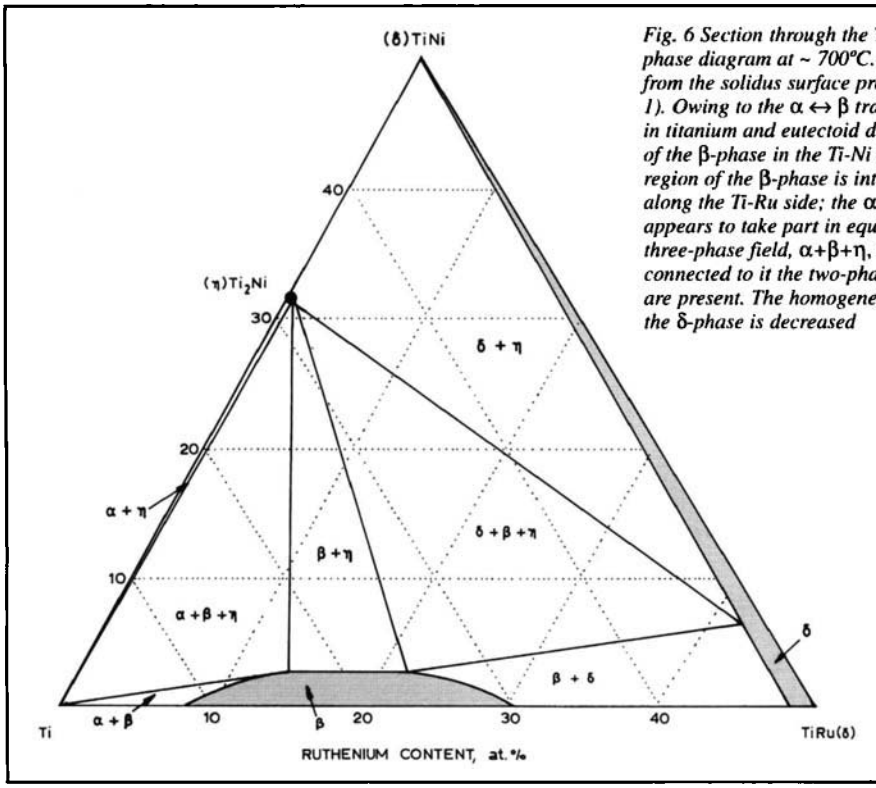

Fig. 6 Section through the Ti-TiNi-TiRu phase diagram at ~ 700°C. It differs from the solidus surface projection (Fig. 1). Owing to the α ↔ β transformation in titanium and eutectoid disintegration of the β-phase in the Ti-Ni system, the region of the β-phase is interrupted along the Ti-Ru side; the α-phase appears to take part in equilibria; a new three-phase field, α+β+η, and connected to it the two-phase field, α+β, are present. The homogeneity interval of the δ-phase is decreased

(maximum temperature 1575°C) through an invariant reaction in the ternary system (980°C) down to an invariant eutectic reaction in the Ti-Ni system (942°C).

Assuming that the polymorphic transformation α ↔ β can occur in titanium and its alloys, it cannot be expected that the phase equilibria on cooling will be the same as they were at the subsolidus temperature. Decreasing the temperature below 882°C should cause changes to the phase equilibria. Figure 6 shows the Ti-TiNi-TiRu phase diagram, deduced at ~ 700°C.

The solubility of ruthenium and nickel in α-titanium is known to be small (< 1 at.% (7)). Therefore the mutual solubility of ruthenium and nickel in α-titanium cannot be expected to be greater than this. This fact, together with the broad homogeneous fields of the β- and δ-phases, and the wide two-phase fields (δ+η, η+β, β+δ) in the solidus surface of the Ti-TiNi-TiRu subsystem, should result in a fine uniform dispersion of α-phase precipitates as well as intermetallic phases within these fields. This in turn should lead to changes in the properties of the alloy, especially in the mechanical properties.

Summing Up

When using or working with new alloy materials, data is required on the processes that take place in the basic alloys, the nature of the processes, their characteristics and the way in which they influence the mechanical properties of the alloys. In general, information about ruthenium-containing alloys is limited. However, alloys based on the compound TiNi in the Ti-Ni-Ru system, may have medical uses, while ruthenium additions to the shape memory alloy TiNi reduce the restoring capability of the alloy, but contribute to repeated reproduction of the shape memory effect. When ruthenium is added to titanium-based alloys, a substantial improvement in corrosion strength occurs in various environments (2). Advantages of using material with a higher corrosion resistance may override any negative effects.

References

1 L. S. Shyriaeva, V. P. Pakhomov, N. G. Boriskina and V. Kasatkin, in "Alloys of Titanium with Special Physical Properties", Moscow, Nauka, 1982
2 R. W. Schutz, *Platinum Metals Rev.*, 1996, **40**, (2), 54
3 J. H. Potgier and H. C. Brookes, *Corros. Eng.*, 1998, **51**, (4), 321
4 K. R. Seddon, *Platinum Metals Rev.*, 1996, **40**, (3), 128
5 E. L. Semenova, N. Yu. Rusetskaya, V. M. Petyukh and V. Ye. Listovnichiy, *J. Phase Equilib.*, 1995, **16**, (4), 297
6 E. L. Semenova, N. Yu. Rusetskaya and V. M. Petyukh, *Platinum Metals Rev.*, 1995, **39**, (4), 174
7 N. G. Boriskina, *Izv. Akad. Nauk USSR, Ser. Met.*, 1983, (2), 222
8 N. G. Boriskina, Inst. Metallurgy of the Akademy of Science of the USSR, Moscow, 1980, Dep. in VINITI 19.11.80, N 4907–80
9 T. B. Massalski, "Binary Alloy Phase Diagrams", ASM, Ohio, 1991

The Authors

Elena Semenova is a Senior Research Worker at the I. N. Frantsevich Institute for Problems of Materials Science, in Kiev. Her interests are transition metal systems, phase equilibria and related properties. She currently studies Cu-Sn-(Ga)-Ti(Zr) alloys.

Nataliya Krendelsberger was a Junior Research Worker at the I. N. Frantsevich Institute for Problems of Materials Science, studying phase equilibria in Ti-Ni-Ru and Ti-Ni-Sc systems.

Ruthenium-Manganese Artificial Photosynthesis Systems

Solar energy is a promising source for sustainable production of fuel and electricity. One way to harvest solar energy is to mimic natural photosynthesis using an artificial system. In plant photosynthesis the key enzyme is Photosystem II, (PSII), where light is absorbed by a chlorophyll unit, starting the conversion of light energy into chemical energy. PSII contains a triad: a cluster of four manganese (Mn) ions which transfer electrons, via tyrosine$_Z$ (a redox active amino acid) to the photooxidised chlorophyll P_{680}^+, which uses the electrons to oxidise water molecules to oxygen. A crucial part of this process is electron transfer from the Mn to P_{680}^+. Light drives electron transport from water to a quinone acceptor which is reduced and used further in bioreactions.

Researchers from Stockholm University, Uppsala University and the University of Lund, Sweden, are currently designing and synthesising multifunctional supramolecular complexes hoping to achieve the light-driven oxidation of water, based on the principles of PSII (L. Sun, L. Hammarström, B. Åkermark and S. Styring, *Chem. Soc. Rev.*, 2001, **30**, (1), 36–49). They have investigated progressively more complex systems. Synthetic multinuclear ruthenium (Ru)-Mn complexes, in which a Ru tris-bipyridine complex replaces the P_{680}, can mimic the electron transfer. A tyrosine unit replaces the tyrosine$_Z$ of PSII. An external electron acceptor accepts an electron transferred by the Ru complex upon absorption of light. The photogenerated Ru(III) then recovers an electron from the Mn cluster or the tyrosine unit and reverts to Ru(II). The Mn cluster has appropriate redox properties and is capable of multiple electron transfer needed for splitting water molecules. The Mn complexes are oxidised or a tyrosine radical is generated. The model system closely mimics the primary reaction steps on the donor side of PSII, but as yet catalytic water oxidation has not been achieved.

The Seventh Grove Fuel Cell Symposium

The seventh Grove Fuel Cell Symposium will take place at the Queen Elizabeth II Conference Centre, London, on 11–13th September 2001. The Symposium, entitled 'Commercialising Fuel Cells: The Issues Outstanding', is intended to give delegates an up-to-date global review of the technology and applications of fuel cells. The major subject areas for discussion will include: stationary fuel cells, transport applications, portable power, defence applications and significant developments in new science and technology.

There will be an extensive poster display and an exhibition area. Further details may be obtained from Ms Sarah Wilkinson, Seventh Grove Fuel Cell Symposium, Elsevier Science, The Boulevard, Langford Lane, Kidlington, Oxford OX5 1GB, U.K. Tel: +44 (0)1865 843691; Fax: +44 (0)1865 843958; E-mail: sm.wilkinson@elsevier.co.uk; Website: www.grovefuelcell.com.

Alfa Aesar All-In-One Catalogue

Alfa Aesar has published its 2001–2002 "Inorganics, Organics, Metals and Materials" catalogue. The 'All-In-One' edition contains Alfa Aesar's entire product range of nearly 25,000 items. A facility on the Alfa website enables platinum labware to be selected and specified in terms of capacity, weight and material. A structure-searchable CD-ROM is also available.

For a free copy of this catalogue, please contact Alfa Aesar, Tel: +1 800 343 0660; Fax: +1 978 521 6350; E-mail: info@alfa.com; Website: www.alfa.com.